

27  
10-3-79  
MASTER

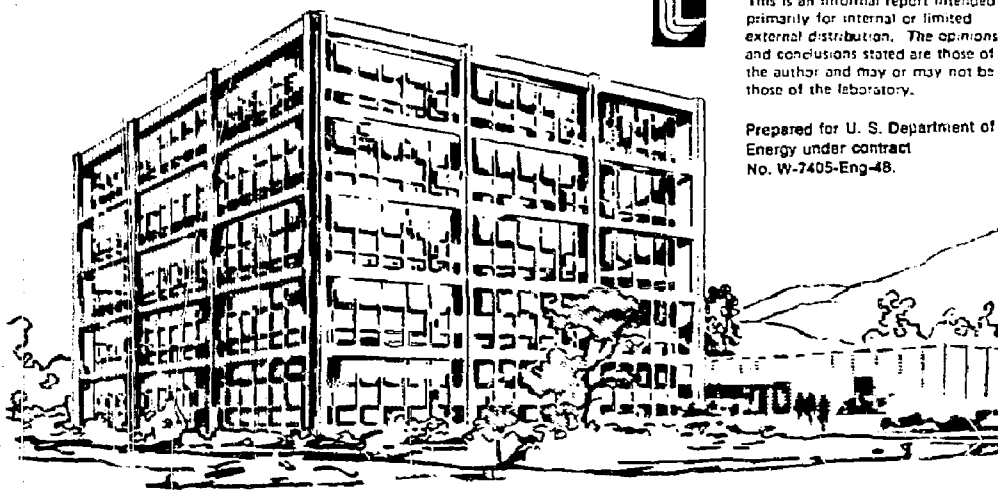
UCID- 18274

# Lawrence Livermore Laboratory

Small-Scale Experimental Tests of Tandem Mirror  
Machines with Thermal Barriers

R. P. Drake

September 1979



This is an informal report intended primarily for internal or limited external distribution. The opinions and conclusions stated are those of the author and may or may not be those of the laboratory.

Prepared for U. S. Department of Energy under contract No. W-7405-Eng-48.

SMALL-SCALE EXPERIMENTAL TESTS OF  
TANDEM MIRROR MACHINES WITH THERMAL BARRIERS

R. P. Drake

NOTICE  
This report was prepared as an account of work sponsored by the United States Government. Neither the United States Government nor any agency thereof, nor any of its employees, makes any warranty, expressed or implied, or assumes any legal liability for the accuracy, completeness, or usefulness of any information, apparatus, product, or process disclosed, or represents that its use would not infringe privately owned rights.

## 1. Introduction

This report summarizes our current physical understanding of tandem mirrors with thermal barriers. Physicists who understand tandem mirrors can use this document as a preliminary guide to the physical issues and experimental problems involved. This report will focus upon the issues that can be tested experimentally, and on the areas needing experimental and theoretical inventions. The next section discusses the plasma potentials and plasma confinement which correspond to a tandem mirror with thermal barriers, assuming the barriers exist in steady-state. Section 3 discusses the creation of a barrier; the natural tendency of the barrier cell to fill with plasma must be countered by pumping ions out of the barrier. Although at present we do not have a satisfactory design for TMX with thermal barriers, a number of important physics issues can be tested in TMX or in smaller experiments. These issues are discussed in Section 4. Section 5 discusses in more detail the design of a barrier-pumping experiment for TMX. The final section summarizes our conclusions and indicates some possible future directions.

## 2. Tandem Mirror Plasma Potentials and Confinement with Thermal Barriers

In a tandem-mirror reactor, the end-plug plasmas must maintain a high electrostatic potential relative to the center cell plasma. This requires large electron temperatures in the end plugs. Because the electrons in the plug were expected to equilibrate quickly with those in the center cell, initial tandem-mirror-reactor designs required a large, constant electron temperature throughout the reactor<sup>(1)</sup>. The discovery and subsequent understanding of electron temperature gradients along field lines in 2XIIB<sup>(2)</sup> made the concept of a thermal barrier possible. The power losses from a tandem-mirror reactor depend strongly upon the center cell electron

17

temperature. A thermal barrier is intended to minimize the conduction of energy from the plug electrons to the center-cell electrons, so as to maintain a relatively low electron temperature in the center cell<sup>(3)</sup>, and to allow other improvements in reactor performance and technology requirements. Any device which decreases the thermal conduction of energy from the end-plug electrons to the center-cell electrons is a thermal barrier. Although this report describes some known thermal barrier designs, we are actively seeking new inventions.

Current thermal-barrier designs minimize the electron thermal conduction along field lines by modification of the plasma potential, as is shown in figure 1. If the plasma potential is decreased by an amount  $\phi_b$  between the end plug and the center cell, the depth of the potential well that confines the plug electrons is increased from  $\phi_c$  to  $\phi_c + \phi_b$ . The center cell electrons are confined in a potential well of depth  $\phi_b$ . Because of the large size of the center cell relative to the plugs, the passing electrons (those which pass through the plugs and the center cell) are maintained at the center-cell electron temperature ( $T_{ec}$ ). Some of these passing electrons leave the plasma along with the departing ions; the associated power loss is proportional to  $T_{ec}$ .

The heat transfer from the plug electrons to those in the center cell is determined by the rates at which 1) plug electrons escape from the plugs into the center cell, 2) passing electrons are trapped in the plug, and 3) collisions in the plug heat the passing electrons. This transfer rate can be determined by a Pastukhov-type calculation, and may be checked by Fokker-Planck calculations. Although our understanding is still evolving<sup>(4)</sup>, a current formula for the conduction power per plug is

$$P_{\text{cond}}(\text{kW}) = \frac{q n_p^2 \frac{\pi}{2} \frac{3}{2} r_p^2 \ell_p (T_{ep} - T_{ec})}{(n\tau)_{ee} \left[ \frac{1}{2} g(R) \exp \frac{(\phi_c + \phi_b)}{T_{ep}} \right]} \quad (1)$$

In this formula,  $n_p$  is the plug density, and  $r_p$  and  $\ell_p$  are the Gaussian radial and axial scale lengths of the plug. The quantity

$n_p^2 \frac{\pi}{2} \frac{3}{2} r_p^2 \ell_p$  resulted from volume integration of  $n_p^2 \exp(-r^2/r_p^2) \exp(-z^2/\ell_p^2)$

and should be modified to perform a single-field-line calculation, or to include the effects of radial variations of electron temperature. The

quantity  $(T_{ep} - T_{ec})$  is the difference between the electron temperature in the plug,  $T_{ep}$ , and that in the center cell,  $T_{ec}$ . The denominator in equation (1) is the characteristic confinement parameter  $(n\tau)$  corresponding to this energy transfer; its precise form remains uncertain. It is clear that the transfer of energy is driven by electron-electron collisions. This contributes the term  $(n\tau)_{ee} (= 5.63 \times 10^8 (T_{ep} \text{ (keV)})^{3/2}$  in TMX with a Coulomb logarithm of 15). The quantity in square brackets converts

$(n\tau)_{ee}$  to the desired  $(n\tau)$ . This quantity is not valid when  $\frac{(i_c + i_b)}{T_{ep}} < 1$ , which may arise in small-scale experiments, so a more accurate analytic expression is being developed. For example, in an ECRH-heated TMX experiment, magnetic confinement of the electrons in the plug may become more important than electrostatic confinement. The quantity  $g(R)$  is

$$g(R) = \sqrt{\pi} \frac{2R + 1}{4R} \cdot n(4R + 2) .$$

Because the feasibility of a thermal barrier depends heavily upon the magnitude of  $P_{cond}$ , experimental tests of equation (1) are very important.

The magnitudes of the potentials depicted in figure 1 are determined by the electron temperatures and densities, the densities being governed by the ion confinement. Fokker-Planck calculations have indicated that  $i_b$  and  $\phi_c$  are determined by Boltzmann-type relations as follows<sup>(5)</sup>:

$$\phi_b = T_{ec} \ln \left( \frac{n_c}{n_b} \right) \quad (2)$$

$$\phi_b + \phi_c = T_{ep} \ln \left( \frac{n_p}{n_b} \right) \quad (3)$$

These relations are valid when  $\frac{1}{2} < \frac{T_{ep}}{T_{ec}} < 2$ , the ultimate limits on their

validity are being evaluated.

Of course, the center cell potential  $\phi_c$  is established to equalize the loss rates of electrons and ions. Ignoring ion losses from the plugs

(as is usually valid), we have

$$\phi_e = T_{ec} \ln \left[ \frac{(n\tau)_c}{\frac{1}{2} (n\tau)_{ee} g(R) \frac{\phi_e}{T_{ec}}} \right] \quad (4)$$

in which the center-cell ion confinement parameter is  $(n\tau)_c$ . The factor of 1/2 which appears in equations (1) and (4) results from the fact that electrons are scattered by ions as well as electrons<sup>(6)</sup>.

The ion confinement determines the densities. Plug ions are lost by familiar processes<sup>(1,7,8,9)</sup>. Center-cell ions are confined by the potential of the end plugs. The confinement parameter, valid in both the collisional and collisionless (Pastukhov) regimes, is<sup>(10)</sup>:

$$(n\tau)_c = (n\tau)_{ii} g(R) \frac{\phi_c}{T_{ic}} \exp \frac{\phi_c}{T_{ic}} + \frac{\sqrt{\pi} n_p \frac{B_p}{B_c} L_c}{v_{ic}} \exp \frac{\phi_c}{T_{ic}} \quad (5)$$

In equation (5),  $(n\tau)_{ii} = 2.5 \times 10^{10} T_{ic} (\text{keV})^{3/2}$ , and  $T_{ic}$  is the center-cell ion temperature. The length  $L_c$  is the effective cylindrical length of the center cell, defined so that the total center-cell volume is  $V_c = L_c \pi r_c^2$ , with  $r_c$  evaluated at the midplane of the center cell. The ion velocity is

$$v_{ic} = \sqrt{\frac{2 T_{ic}}{M_c}} = 4.4 \times 10^7 \sqrt{T_{ic} (\text{keV}) / M_c (\text{AMU})}.$$

The confinement of ions in the barrier cell is the subject of the next section.

The addition of a barrier cell to a tandem mirror effectively decouples the plasma potential from the plug density. This means it is possible in principle to maintain electrostatic confinement of center cell ions with a comparatively small density in the end plug. In small experimental tandem mirrors, the difficulties imposed by stability and vacuum conditions severely limit the densities and potentials which can be

obtained. However, small experiments can test a number of physics issues which are crucial to the success of thermal barriers, as is discussed in section 4. In reactors, the addition of thermal barriers introduces a trade-off between the technological sophistication and power input required to maintain the end plugs and those needed to maintain the barriers.

### 3. Ion Confinement in Thermal Barriers

#### A. Filling of Thermal Barriers

A barrier cell will fill up unless it is pumped. It is well known that multiple-mirror systems containing Maxwellian plasmas equilibrate to uniform density. The effect of a non-Maxwellian center-cell density on the potential inside the barrier is discussed at the end of this section. Assuming the center-cell plasma is Maxwellian, the barrier density can be decreased by pumping ions out of the barrier faster than they are trapped by collisions. The filling and pumping of the barrier cell will be discussed in turn.

Collisions trap particles in the barrier cell, as is illustrated in figure 2. The Maxwellian center cell produces a constant flux of passing ions. These particles have a characteristic random energy  $T_{ic}$  and a directed velocity resulting from the potential through which they have fallen. The density of passing ions,  $n_{pass}$  is:

$$n_{pass} = \frac{n_c}{R_b} \sqrt{\frac{T_{ic}}{\pi\phi_b + T_{ic}}} \quad (6)$$

Here  $R_b$  is the mirror ratio of the barrier ( $B_{mb}/B_b$ ). These ions are trapped as the result of collisions which change their velocity or reduce their energy. Small-angle scattering traps passing ions magnetically; they are scattered out of the loss cone. Diffusion downward in energy causes ions to become electrostatically trapped (deeply trapped). The fluxes corresponding to these two types of trapping are indicated in figure 2.

Some limits may easily be placed on these trapping rates. Analytical analysis and numerical computations are increasing our ability to model them in detail. In the limit of a completely empty barrier, a large mirror ratio  $R_b$ , and the consequent large potential  $\phi_b$ , the trapped current per

unit volume can be estimated. The trapping rate due to small-angle scattering will be

$$j_a = 2 \frac{(n_{\text{pass}}/2)^2}{(n\tau)_a} .$$

In this limit each group of passing ions (see Fig. 2) interacts primarily with itself, because the relative velocity of the two groups of passing ions is high. The quantity  $(n\tau)_a$  may be taken as  $(n\tau)_a = (\Delta\theta)^2 (n\tau)_{ii} = 2.5 \times 10^{10} T_{ic}^{3/2} / R_b$ . The deep trapping rate (due to diffusion in energy) is estimated from Fokker-Planck calculations to be

$$j_d = \frac{n_{\text{pass}}^2}{5.5 \times 10^9 T_{ic}^{3/2}} .$$

From these calculations the total trapping rate in this limit is,

$$j_1 (\text{cm}^{-3} \text{s}^{-1}) = \frac{n_{\text{pass}}^2}{2.5 \times 10^{10} T_{ic}^{3/2}} \left( \frac{R_b}{2} + 4.55 \right) (\text{cm}^{-3}, \text{keV}). \quad (7)$$

Because no real barrier cell will be completely empty, equation (7) should place a lower limit on the trapped current, subject to more accurate calculations of the deep trapping term.

When the barrier cell is partially full, passing ions will be trapped by collisions with trapped ions as well as with themselves. In this case the trapping rate is enhanced by an amount  $2g_b = 2(n_b/n_{\text{pass}})$ , because the density of scattering centers is now  $n_b$  rather than  $1/2 n_{\text{pass}}$ . Ignoring the detrapping of ions already trapped in the barrier cell, we obtain as an upper limit on the trapping rate

$$j_2 = \frac{2g_b n_{\text{pass}}^2}{2.5 \times 10^{10} T_{ic}^{3/2}} \left( \frac{R_b}{2} + 4.55 \right) . \quad (8)$$

The quantity  $g_b$  represents the amount of filling of the barrier, with  $g_b = R_b$  when  $n_b \approx n_c$ . However,  $g_b$  is not proportional to

$\frac{n_b}{n_c}$  because of the effects of the barrier potential  $\phi_b$  (see Eq. 6).

Because the two limits derived above are quite different, a better expression for the trapping rate is needed, and experimental studies of this type of transport in velocity space would be helpful. Recent Fokker-Planck computer-code calculations have led to the expression

$$j_{\text{trap}} = \frac{n_{\text{pass}}^2}{2.5 \times 10^{10} T_{ic}^{3/2}} (2.5 R_b + 4.55), \quad (9)$$

which is used below. However, this expression will probably be revised once some numerical difficulties have been overcome.

#### B. Pumping of Thermal Barriers

To pump a thermal barrier is to remove ions from it. It would seem easy to attain poor ion confinement, but a simple, inexpensive, technologically feasible and theoretically tractable idea has not yet emerged. The more promising schemes are reviewed below.

Neutral beams can be used in two ways to pump ions from a barrier. Both schemes depend upon replacement by charge-exchange of trapped ions in the barrier with untrapped ions provided by the beams. The trapped ions escape the plasma after they are neutralized. Both types of neutral-beam pumping are illustrated in figure 3. First, a neutral beam can be injected nearly parallel to the magnetic axis, so that the ion produced by charge-exchange becomes a passing ion. Second, a relatively energetic beam can be injected perpendicular to the magnetic axis, so that the resulting ions have very large orbits and can be removed by a limiter, charge-exchange outside the plasma, or radial diffusion. In both cases, ionization of the beam or charge-exchange on passing ions do not tend to fill the barrier. The first technique is probably best for a reactor; the second may be easiest to use in a small-scale experiment.



The principal advantage of neutral-beam pumping is that all the ions in the barrier can be pumped by this technique. Proper choice of beam energy and aiming allows the beams to interact strongly with any desired class of particles. The disadvantages of neutral-beam pumping is that it is not very efficient. The neutral beams chosen must have sufficient velocity to penetrate the plasma and sufficient current to maintain a large neutral density within the plasma. In a neutral-beam-pumped-barrier machine, this power input becomes the dominant one. In application the beams may be used only to pump the deeply trapped ions, which are hard to reach by other techniques.

A gas box can be used to pump magnetically trapped ions, by replacing them with passing ions. Figure 4 illustrates this idea. At the gas box, which is located in the elliptical quadrupole fan, plasma ions are replaced by gas box ions of negligible energy. When these cold ions reach the barrier midplane, they are passing ions because of the energy they have acquired from the plasma potential. The gas box pumps the barrier by charge-exchange of trapped ions, fuels the center cell by ionization, and costs additional power by charge-exchange of passing ions.

Gas-box pumps have the advantage that they are cheap and easy to build. However, they cannot completely pump out a barrier. A gas-box cannot pump deeply trapped ions, which never reach it. This means that gas box pumping must be supplemented by some other technique. In addition, the penetration of the gas into the plasma is inefficient, even in the elliptical magnetic fan. This will lead to enhanced power loss and greater vacuum problems.

Jay Kesner<sup>(11)</sup> has suggested that particle drifts might aid in pumping out a barrier. The essential point is that particles in a barrier drift across magnetic flux surfaces, and when they have drifted outside of the plasma flux tube defined by the plug plasma size, they are accessible to a limiter or to charge-exchange pumping. The magnetic drift surfaces in a barrier cell which joins a quadrupole plug field to a circular solenoid field enable such pumping. This effect could be enhanced by careful magnet design.

Although it is clear that particle-drift effects can help remove particles from a barrier, drift-surface pumping has limitations and difficulties. First, this technique has difficulty pumping ions trapped in

the core of the barrier, which tend not to drift outside of the plasma flux tube. As such ions are the most important, drift-surface pumping at its best must be supplemented. Second, the actual particle drifts result from electric fields as well as magnetic fields, and are difficult to determine using current theory. This means that it is difficult to predict when these effects will become significant. Third, the limiter or gas used to pump the barrier impose difficult impurity and vacuum problems, especially in a small-scale experiment.

Another technique that has received some attention is magnetic decompression. A large magnetic field is created in the barrier cell, and the density there equilibrates to the center-cell value. Then the barrier field is decreased very rapidly. This decompression decreases the density in the barrier cell much faster than the trapping rate increases it. The density depression relative to the center cell lasts until the barrier fills in. This technique appears technically unsuitable for reactors, but it might be used in smaller experiments to study the filling rate of barrier cells. For example, in TMX a single-turn coil voltage of order 40 kV would be required to create the barrier cell in roughly  $10^{-5}$  sec, and the barrier would be expected to fill in within  $10^{-3}$  sec. An even smaller experiment might be able to address the problem of barrier filling in detail.

Various pumping schemes using radio-frequency electromagnetic fields have also been proposed. One such idea uses an rf field to adiabatically reflect ions from a local region of high magnetic field, thereby creating a potential well.<sup>(12)</sup> Theoretically it appears that this will work. However, the rf fields required to create a barrier in a reactor are unfeasibly large. It appeared that magnetic field fluctuations might be used to jostle ions out of the barrier,<sup>(3)</sup> but Monte Carlo calculations indicated that the magnetic-field fluctuations required were too large (of the order of the initial field in the barrier cell). It is likely that rf fields could be used to help pump a barrier cell, but a technically feasible and theoretically tractable scheme has not been found. A clever, scalable experiment would be very helpful.

It has become clear that although some workable pumping methods have been invented, more and better ideas are definitely needed. The efficiency with which a barrier cell can be pumped is the most important factor which determines the performance of a tandem mirror reactor with barriers.

### C. The Effect of an Anisotropic Center-Cell Plasma

A potential well can be created in a barrier cell (or at an extremum of the magnetic field) if the plasmas in the adjacent regions are non-Maxwellian. In a tandem mirror, the density in the barrier cell will equilibrate with the Maxwellian component of the plasma in the center-cell. If the center cell is beam-heated or rf-heated so as to create a magnetically-confined, non-Maxwellian plasma, a potential well will be created. The barrier density will then increase until the currents into and out of the barrier are equal. A steady-state potential well will develop.

The magnitude of this potential well can be estimated by assuming the center cell density ( $n_{ce}$ ) to be composed of cold, Maxwellian ions ( $n_{cc}$ ) and hot, magnetically-confined ions ( $n_{ch}$ ). Then

$$n_{ce} = n_{cc} + n_{ch}$$

$$\phi_b = T_{ec} \ln \left( \frac{n_{ce}}{n_b} \right)$$

$$\Gamma_b A_b = \Gamma_c A_c$$

Here  $\Gamma_b A_b$  is the particle flux out of the barrier times the area of the barrier.

The barrier area is  $A_b = A_c \frac{B_c}{B_b}$ . Because the potential drop occurs within the center cell, the particle current leaving the barrier is

$$\Gamma_b A_b = \frac{n_b}{2} \frac{\sqrt{2T}}{R_b} \quad , \quad \Gamma_c \frac{B_c}{B_b} = \frac{A_c}{R_c} \frac{n_b}{2} \sqrt{\frac{2T}{\pi m}} \quad .$$

The current leaving the center cell may be found by integrating over the loss cone of the Maxwellian plasma, which gives

$$\Gamma_c A_c = \frac{A_c}{R_c} \frac{n_{cc}}{2} \sqrt{\frac{2T}{\pi m}} \left[ R_c - (R_c - 1) \exp \frac{-\phi/T}{R-1} \right] \quad .$$

Setting these currents equal, we obtain

$$n_b = n_{cc} \left[ R_c - (R_c - 1) \exp \frac{-1/T}{R_c - 1} \right]$$

and from the above this gives

$$\frac{\gamma}{T_{ec}} = n \left( 1 + \frac{n_{ch}}{n_{cc}} \right) = n \left[ R_c - (R_c - 1) \exp \frac{-1/b \cdot T_{ic}}{R_c - 1} \right]. \quad (10)$$

Supposing  $R_c = 10$ ,  $n_{ch} = 2n_{cc}$ , and  $T_{ic} = 1/2 T_{ec}$ , then  $b = .4 T_{ec}$ .

The above estimate shows that a non-Maxwellian center-cell plasma does result in a steady state potential well, which will decrease the thermal conduction between the plug and the center-cell. However, either a very large center-cell mirror ratio or an extremely anisotropic and possibly unstable center-cell plasma would be required to obtain the desired potential well of several times  $T_{ec}$ .

#### 4. Physics Issues Which Can Be Investigated

The above sections have considered how a thermal barrier works and how one might be created. Current thermal barrier designs can be fully tested only in large experiments, because of the plasma volumes, energies, and densities involved. However, the feasibility of a thermal barrier rests on a number of physical theories and technical assumptions and many of these can be tested in TFX and in smaller laboratory experiments. This section reviews some of these issues and possible tests of them.

##### 4. Thermal Conduction

The concept of a thermal barrier rests on the finite thermal conduction of energy along field lines by the electrons. The magnitude of this conduction in large part determines its effectiveness. Good experimental tests of the magnitude and scaling of the electron thermal conduction are therefore very important. In such tests, a known amount of power will be made to flow from one group of electrons to another group of

electrons. The magnitude and the scaling of the resulting temperature difference will be measured.

These experiments are possible in TMX, particularly after the addition of ECRH heating. The expected temperature differences ( $T = T_{ep} - T_{ec}$ ) in TMX without ECRH are illustrated in figure 5, as a function of plug ion density and mean energy. The center cell density is assumed to be  $10^{13} \text{ cm}^{-3}$ , in order to measure  $T_{ec}$  by a conventional Thomson scattering system. The curves in figure 5 were obtained by equating the power input to the plug electrons (by Spitzer drag) with the power conducted to the center-cell electrons are given by equation (1). Without ECRH, TMX cannot be expected to produce temperature differences large enough to test the theory of electron thermal conduction, unless either 1) the theory significantly overestimates the conduction or 2) TMX creates its own thermal barrier by some mechanism, perhaps related to rf fluctuations.

Figure 6 illustrates the magnitude of the temperature differences  $T$  which could be obtained using ECRF heating. The temperature differences shown in figure 6 are indicative rather than predictive; they are based on partial model of the plasma dynamics. The point of the figure is that measureable and variable temperature differences should be obtained with the absorption of a few hundred kw of ECRH power. Similar temperature differences have been predicted by Steve Devoto, using a self-consistent point-model computer code.

### B. MHD Stability

The addition of a barrier cell to a tandem mirror adds new regions of unfavorable field-line curvature which may adversely affect the MHD stability of the device. Considering figure 1, it is clear that the barrier mirror creates unfavorable curvature where the center-cell plasma pressure may be significant. Calculations have shown that the new field designs should be stable to the flute-interchange instability, but they appear to have very poor stability with regard to the ballooning mode.<sup>(13)</sup> However, these theoretical calculations have not been experimentally tested, and are somewhat open to questions because they are exact only in the limit of infinite wave number (zero wavelength) perpendicular to B. An experimental test of MHD theory, to what ever extent is possible, would be quite useful.

We are investigating whether we can create a significantly unstable plasma in TMX with the existing coils and power supplies or after minor

modifications. This will allow a test of interchange theory, and possibly of ballooning theory. However, the higher plasmas created in TMX will have significant ion-Larmor radii, and should be more stable than the models predict. We will be able to place limits on reactor stability, bounded by TMX and infinite-wavenumber theory, but the precise stability limits will be difficult to discern. Other experimental tests of MHD theory are also needed.

#### C. Barrier Filling and Pumping

As was discussed in section 3, it is also difficult to predict the rate at which passing ions are trapped in a barrier. Experimental studies of this issue would be useful, especially if they could measure the deep trapping and magnetic trapping rates as a function of how full the barrier is. Two basic approaches might be used; they will be briefly discussed.

First, an empty barrier cell could be created by rapid magnetic decompression, and the trapping rates could be deduced from density measurements. This experiment would be difficult using TMX, because of the high collisionality of the center cell and poor diagnostic access. The filling rate of the barrier could be estimated, but detailed study of the scaling of the trapping rates would be difficult. A university-scale experiment using lower densities and lower magnetic fields could be a good way to study this issue. The results of such an experiment, if it was well-designed, would enhance our understanding of many velocity-space-diffusion processes. For example, the theory of electron thermal conduction requires an understanding of such processes.

Second, a steady-state barrier cell could be pumped by "well-understood" techniques. The scaling of the barrier density might reveal the magnitude of certain trapping rates. Unfortunately, the trapping rates inferred from the data will be model-dependent and will not be very precise. Such an order-of-magnitude measurement of the trapping rate would be better than no measurement of it, but a more informative experiment is desirable.

A final set of issues which can perhaps be addressed in small experiments are the techniques of pumping ions out of a barrier cell. In section 5, the feasibility of pumping a barrier cell in TMX is examined as an example. Neutral-beam pumping will undoubtedly work, but is difficult to test in a low-power, small-plasma experiment. Gas-box pumping might be

investigated, to determine whether complications arise due to poor gas penetration or other causes. Experiments that investigate particle drift surfaces might aid the evaluation of drift-surface pumping, especially if they could investigate the effects of electric fields. Finally, an experimental demonstration and theoretical account of a scalable RF pumping technique could be a major advance in tandem-mirror technology.

#### 5. A TMX Thermal Barrier Design

This section summarizes our efforts to design a thermal barrier experiment in TMX. This design effort provided useful knowledge regarding barrier pumping and magnet design. Present designs indicate a barrier-pumping experiment might be performed, but that the overall performance of TMX would not improve. New design approaches are needed to improve TMX performance with thermal barriers.

##### A. A Thermal-Barrier-Enhanced TMX?

A thermal barrier enhances the ion confinement in a tandem mirror by allowing a larger plug potential for the same power input; this permits an increase of the center-cell density or other equivalent improvements. However, in TMX the center cell ion confinement is determined by the need to stabilize the end plugs. If a thermal barrier in TMX allowed a higher plug potential, more stabilizing current would be needed. This conflicts with the desired improvement in ion confinement, and in addition the center cell density cannot be increased because of the need to minimize the filling rate of the barrier cell. To make matters worse, the addition of two barrier cells to a center cell which is already small reduces the center cell volume substantially. In sum, adding thermal-barrier cells to TMX in this way would decrease the ion confinement in order to maintain plug stability through plasma loss from a smaller central cell plasma volume. We need to discover a way to maintain steady-state end plugs without stabilizing current or strong electron cooling, and ways to make thermal barriers more compact to fit into TMX.

Because of the above considerations, we have considered the addition of one barrier cell to TMX, to demonstrate barrier pumping. Such an experiment would attempt to show a reduction in barrier density and possibly to measure the creation of a potential well. This design and its performance are discussed below.

## B. Field Design

Figure 7 illustrates one TMX field design for a thermal-barrier cell. This design uses one additional mirror coil to create the barrier mirror. Although the flux tube is not very circular in the center cell (the deviation from a circular cross-section is 23%), a barrier with  $R_b = 10$  is created with minimal modifications to the experiment. We have obtained a more circular field design by replacing the octupole coil in TMX with a negative-curvature-negative-current bucking coil (Fig. 8). Note in figure 7 that the center-cell volume is the half of the machine with the barrier is very small. The interchange-stability limit of this field design is  $\beta_c = .26\beta_p$ . A summary of these field designs and their characteristics may be obtained. (14)

## C. Barrier Filling

The barrier filling rate limits the allowable center-cell parameters. Using equations (6) and (9) and integrating over the barrier volume, one can obtain

$$I_{\text{trap}} \sim 73 \frac{q \pi r_c^2 \sqrt{1 - \beta_c}}{5.5 \times 10^9 R_c} \frac{n_{cc}^2}{T_{ic}^{3/2}} \quad (11)$$

In this relation  $n_{cc}$  is the Maxwellian component of the center-cell plasma and  $T_{ic}$  (keV) is its temperature. Using  $r_c = 16$  cm,  $\beta_c \sim 0$ , and  $R_c = 6$  gives the following table:

Table 1. Barrier Filling Estimates in TMX

Trapped Current in amps vs  $n_{cc}$ ,  $T_{ic}$

$T_{ic}$ (keV)	.1	.3	.5	1
$n_{cc} (10^{13} \text{ cm}^{-3})$				
1	910	170	80	30
2	3600	700	330	120
3	8100	1600	700	260
5		4400	2000	710



As will be seen below, it is not feasible to pump hundreds of amps out of a TMX barrier cell. The base-case TMX center cell is very collisional and the barrier fills in very fast. The only operating point which might allow the barrier to be pumped is  $n_{cc} = 10^{13} \text{ cm}^{-3}$ ,  $T_{ic} = 500 \text{ eV}$ . This would require substantial heating of the center-cell ions, and scaling experiments of pumping and trapping probably would not be possible. ( $n_{cc}$  cannot be lowered below  $10^{13} \text{ cm}^{-3}$  because of the needs to stabilize the end plugs, and to measure  $T_{ec}$  with a Thomson scattering system.) On the assumption that the operating point described above could be achieved, the pumping of this current will be examined next. Note that equation (9) was an estimate, and that the actual trapping rate could be significantly smaller or larger than table 1 suggests.

#### D. Barrier Pumping

The pumping required to remove 80 amps of trapped current from a barrier must pump both deeply and magnetically trapped ions, in the core of the barrier as well as on the surface. A combination of neutral-beam and gas-box pumping is evaluated here. Drift surface pumping was evaluated using particle drifts computed by Jim Foote. The core of the plasma (radius  $\leq 8 \text{ cm}$ ) cannot be pumped by this technique. However, the outer edges of the plasma could lose a significant current due to this effect.

As discussed in Section 3, the deeply trapped ions must be pumped by the neutral beams. For  $R_b = 10$ , this current is roughly 17% of the total current, or 13 amps in this case. However, because some magnetically-trapped ions will also be pumped, the total neutral-beam pumping must be roughly 20 amps. In the thin plasma limit, which underestimates the required neutral beam current, we have

$$I_{(\text{beam pump})} = I_{\text{beam}} \sigma_{cx} n_b r_b \sqrt{\pi}.$$

Taking  $\sigma_{cx} = 10^{-15} \text{ cm}^2$ ,  $n_b = 1/2 n_c = 5 \times 10^{12} \text{ cm}^{-3}$ ,  $r_b = 19 \text{ cm}$ , and  $I_{(\text{beam pump})} \approx 20 \text{ amps}$ , we obtain  $I_{\text{beam}} = 120 \text{ amps}$ . This can be supplied with three beams in top operating condition. Because of attenuation by the plasma and availability, four beams are probably required.

In addition to the neutral-beam pumping, the gas box must pump 60 amps of trapped ions, replacing them with passing ions by charge-exchange. If the gas box is located where B is half the mirror field, the trapped region

is about 70% of the total available phase space. We estimate the pumping rate as

$$60 \text{ amps} = q L_{gb} A_{gb} n_{gb} n_o \langle cv \rangle_{cx} \times .7 .$$

Using the gas box area  $A_{gb} = 230 \text{ cm}^2$ , gas box length  $L_{gb} = 15 \text{ cm}$ , gas box density  $n_{gb} = 10^{13} \text{ cm}^{-3}$  and  $\langle cv \rangle_{cx} = 2 \times 10^{-8} \text{ cm}^3 \text{ s}^{-1}$ , we obtain a neutral density within the plasma in the gas box,  $n_o = 8 \times 10^{11} \text{ cm}^{-3}$ . This density is easily obtainable, on the basis of previous experience with gas boxes in TMX and 2XIIB. The potential of the gas box is above that in the center cell because the electron temperature is higher in the plug (if necessary, ECRH heating would be used). Thus, a combination of neutral-beam pumping and gas-box pumping might succeed in reducing the density in a barrier cell in TMX. The crucial uncertainty in this case is just how much neutral-beam pumping is needed to handle the deeply-trapped current while at the same time satisfying center-cell heating and vacuum requirements.

## 6. Conclusion

Although the experiments designed thus far do not improve TMX parameters, they can test several physics issues which are crucial to the success of a thermal barrier. TMX can test the theory of electron thermal conduction along field lines and, to some extent, MHD stability theory. TMX might be able to test barrier filling rates and barrier pumping, within a degree of uncertainty. Smaller experiments could very usefully examine barrier filling, MHD stability, and new pumping techniques, especially those involving rf fields.

Beyond this, the basic concept of the thermal barrier is still a ripe subject for inventions. For example, we are examining the use of a barrier cell and a simple mirror added onto a basic tandem mirror. The quadrupole field in the basic tandem mirror would provide MHD stability, and would reduce the current into the barrier (and hence the trapping rate) to more manageable levels. The outer mirror would be thermally isolated from the rest of the machine and ECRH would be used to provide a very high potential barrier. This scheme, and quite possibly others, may enhance the usefulness of the thermal barrier. But no matter what develops, the basic experiments discussed above will be applicable to all thermal barriers.

#### ACKNOWLEDGEMENTS

The work described in this document contains the efforts of a significant fraction of the physicists in M-division at Lawrence Livermore Laboratory. The field designs and engineering studies were done by Bob Wong, Buzz Pedrotti, and Tony Chargin, with substantial assistance from other engineers. I'd especially like to thank Grant Logan, Tom Simonen, and Dave Baldwin for insights and assistance.

# REFERENCES

1. R. W. Moir, et al., "Preliminary Design Study of the Tandem Mirror Reactor," LLL report UCRL-52302 (July, 1977).

For improved reactor studies without thermal barriers, see G. A. Carlson, B. M. Boghosian, J. H. Fink, J. O. Myall, W. S. Neef, Jr., "Parametric Studies of Tandem Mirror Reactors," LLL internal report UCID-18158 (April, 1979).

2. J. F. Clauser, "Power Balance and Electron Temperature in 2XIIB," Bull. Am. Phys. Soc. 23, 850 1978.

3. D. E. Baldwin, B. G. Logan and T. K. Fowler, "An Improved Tandem Mirror Fusion Reactor, UCID-18156, April 1979.

4. R. H. Cohen, LLL, private communication, September 14, 1979.

5. D. E. Baldwin, LLL, private communication, September 14, 1979.

6. R. H. Cohen, M. E. Rensink, T. A. Cutler, A. A. Mirin, Nucl. Fusion 18 (1978) 1229.

7. Baldwin, D. E., Rev. Mod. Phys. 49 (1977) 317.

8. F. H. Coensgen and T. C. Simonen, "Magnetic Mirror Confinement of High-Energy, High-Density Plasma," UCRL-82790, August 1979.

9. W. C. Turner, Journal de Physique, Colloque C6, Suppl. 12, Tome 38, C6-121 (1977).

10. T. Rognlien and T. Cutler, private communication, Nov. 22, 1978 (MFE memo MFE/TC/78-399)

11. J. Kesner, "Passive Generation of Ambipolar Potential Barriers in a Tandem Mirror," University of Wisconsin, LLWFDM-303, 1979.

12. Y. Matsuda and D. E. Baldwin, Mirror Theory Monthly (LLL), Aug. 15, 1979.

13. T. Kaiser, LLL, private communication, September 15, 1979.
14. R. Wong, L. Pedrotti, A. K. Chargin, and R. P. Drake, LLL Internal Memo, 1979.

FIGURE CAPTIONS

1. Magnetic fields, plasma potentials, and plasma densities in a tandem mirror with a thermal barrier. The plug density  $n_p$  may or may not be greater than the center-cell density  $n_c$ .
2. Passing ions flow through the barrier cell. They become deeply trapped by diffusing to lower energy or magnetically trapped by scattering in angle.
3. A neutral beam nearly parallel to the machine axis replaces trapped ions with passing ions by charge-exchange (1). Cross-field injection of energetic beams can replace trapped ions with ions whose orbits leave the plasma (2).
4. Gas-box pumping replaces magnetically trapped ions with passing ions.
5. Predicted electron temperature differences  $\Delta T$  between the plug and the center cell in TMX without ECRH heating, depending on plug density and mean ion energy.
6. Indicative temperature differences  $\Delta T$  which could be obtained using ECRH heating in TMX.
7. A magnetic field plot showing the addition of a barrier cell to TMX.
8. An improved magnet set to create a barrier cell in TMX, using a reverse-curvature reverse-current transition coil.

# THERMAL BARRIER

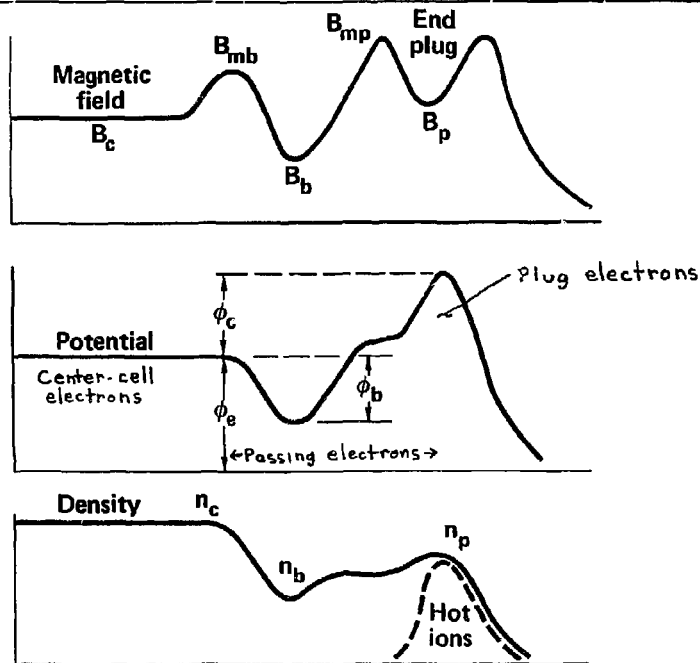


Figure 1

# Velocity Space at Minimum Barrier Field

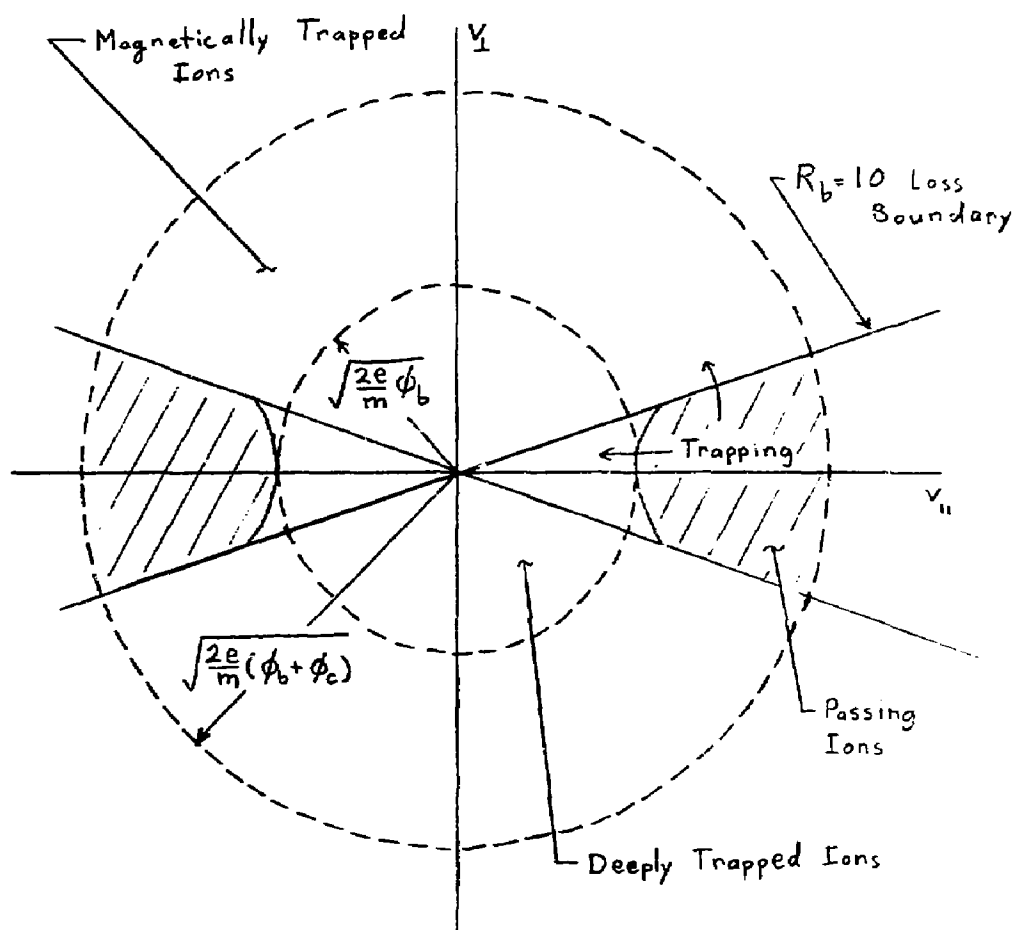
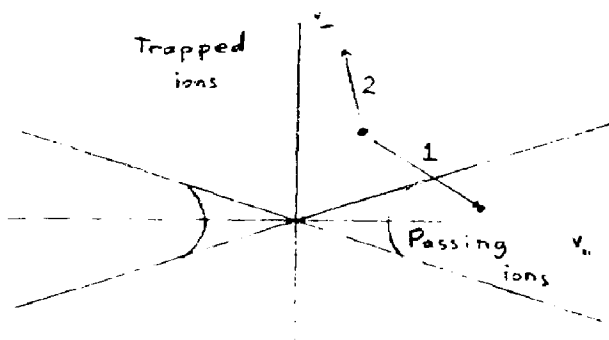


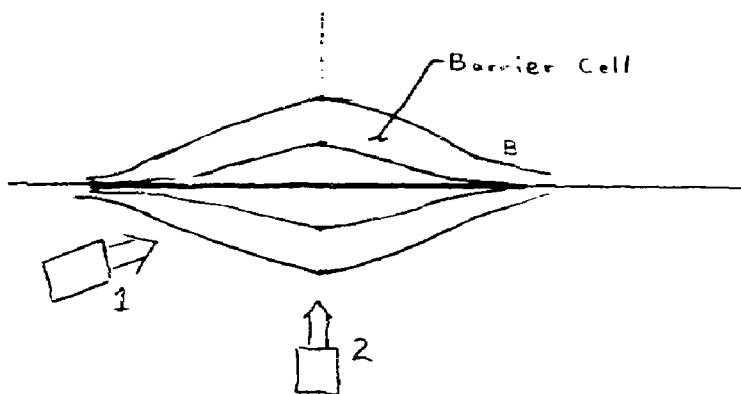
Figure 2



# Neutral Beam Pumping



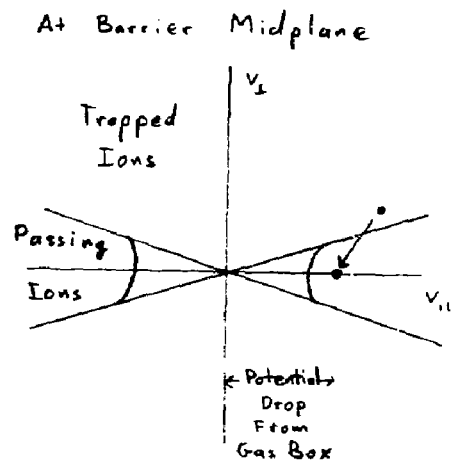
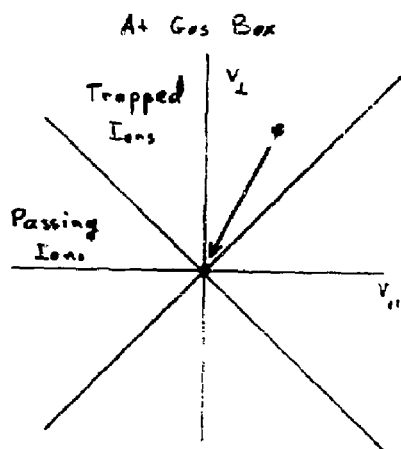
## Velocity Space



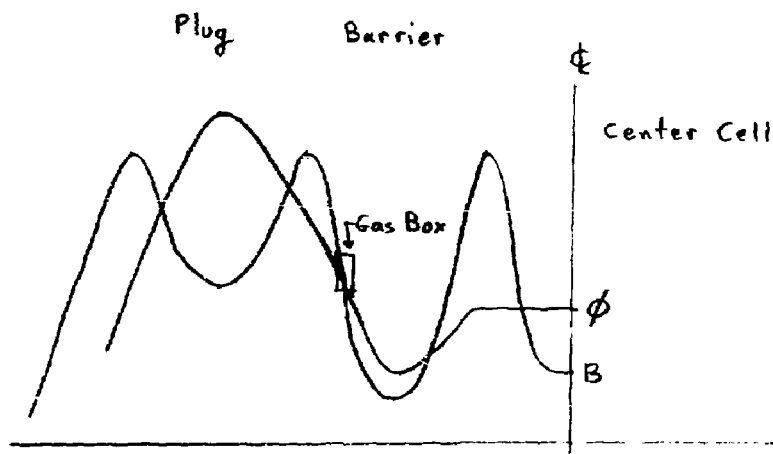
## Neutral Beam Locations

Figure 3

# Gas Box Pumping



velocity Space



Sketch of Machine

Figure 4

# TEMPERATURE DIFFERENCES IN TMX BASE CASE

RPD 9/4/79

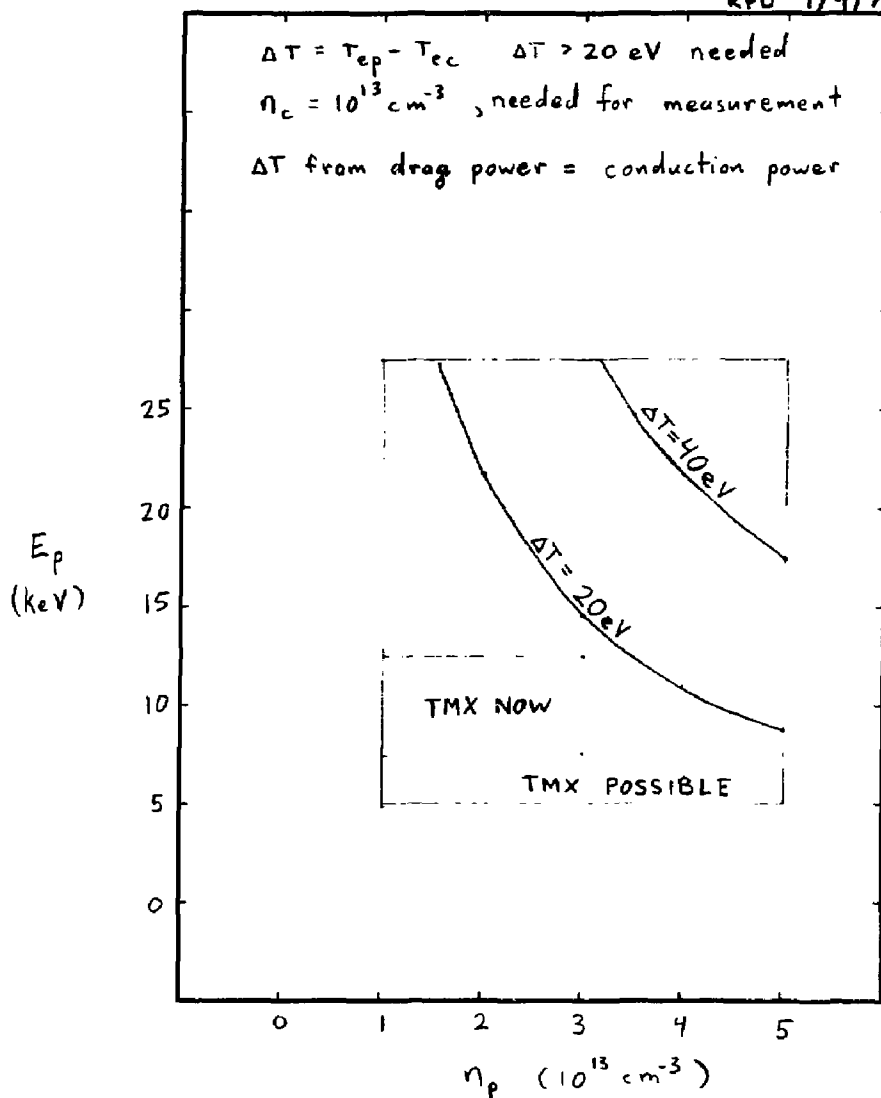


Figure 5

# EFFECTS OF ECRH HEATING OF EAST PLUG REV. 1

RPD 9/5/79

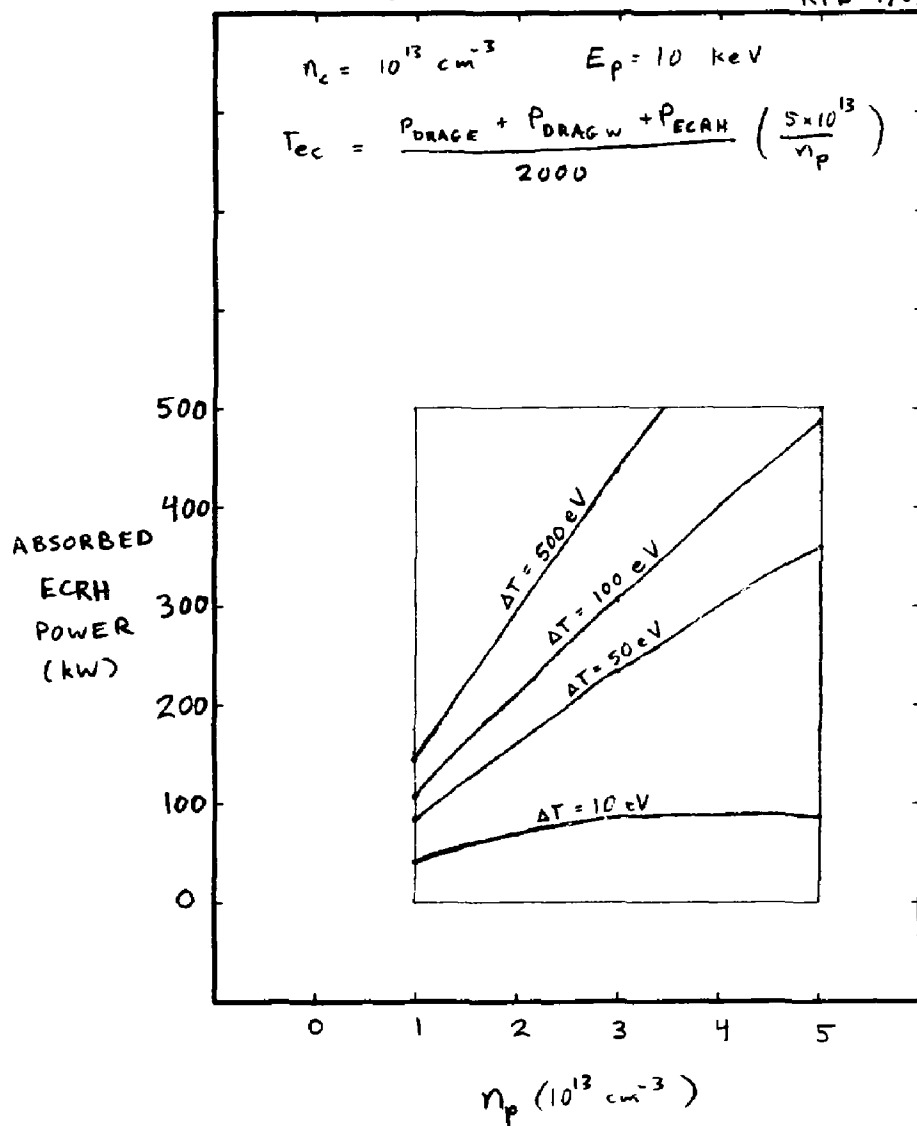


Figure 2.6

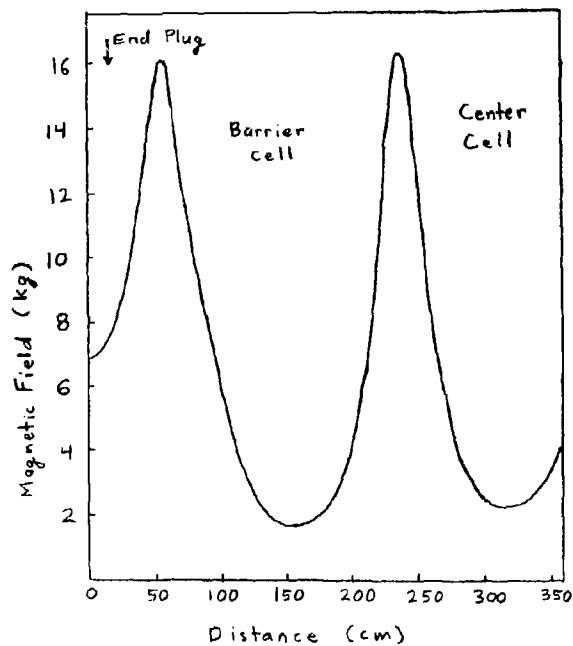


Figure 7

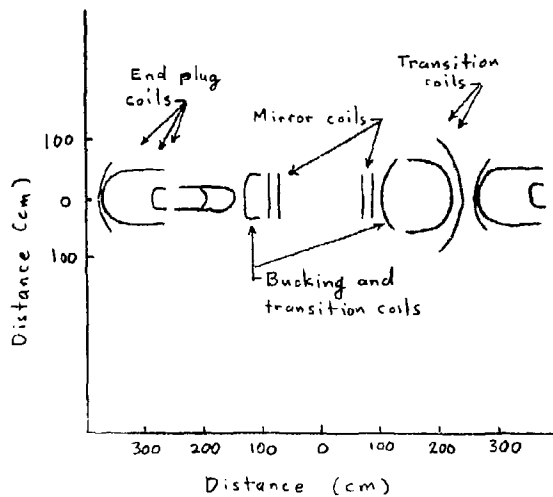


Figure 8